Thermo-mechanical studies of highly oriented poly(ethylene terephthalate)

U. Göschel*
Max-Planck-Institute for Polymer Research, W-6500 Mainz, Germany
(Received 16 April 1991; accepted 17 June 1991)

Highly oriented poly(ethylene terephthalate) samples of different supermolecular structures obtained by a uniaxial drawing process were investigated by means of static stress–strain experiments, relaxation experiments and dynamic-mechanical experiments. The influences of strain and temperature on the time-dependent mechanical properties were used to characterize the dynamical behaviour of these structures and to find relations between the known supermolecular structure and the molecular mobility.

(Keywords: highly oriented poly(ethylene terephthalate); supermolecular structure; time-dependent mechanical behaviour; chain slippage)

INTRODUCTION

The uniaxial drawing technique is a useful method for preparing highly oriented poly(ethylene terephthalate) (PET) films. In general, high chain orientation is accompanied by high axial elastic modulus (E) in the drawing direction. The preparation of such samples by using a multi-stage combined drawing/hot zone drawing procedure has been described previously[1]. Samples obtained showed a high orientation of the macromolecules, expressed by a birefringence of $0.177 \leqslant \Delta n \leqslant 0.249$, and a high E of $7.1\ \text{GPa} \leqslant E \leqslant 16.8\ \text{GPa}$. The supermolecular structure of these samples was intensively investigated by using WAXS and SAXS[2]. The influence of supermolecular structure on the axial modulus and on the limitations in preparing high modulus PET were discussed.

The present paper continues the above investigations and describes the thermo-mechanical behaviour of the above supermolecular structures on the basis of molecular mobility. Such investigations also contribute to a better understanding of the mechanism of the structure formation processes which occur during drawing.

EXPERIMENTAL

Preparation of samples

PET samples ($M_w \sim 20000$) with an amorphous structure, as seen by X-ray, and nearly isotropic ($\Delta n \leqslant 0.5 \times 10^{-3}$), and with a thickness of 180 μm and a width of 2.8 mm, were uniaxially drawn using various conditions[1] to obtain different supermolecular structures with a high chain orientation. These structures were characterized by static mechanical investigations, optical birefringence[1] and WAXS and SAXS[2]. The data obtained are shown in *Table 1*. The designation of the samples corresponds to that in previous studies[1,2]. Samples 1 and 8 are non-crystalline, but highly oriented. Samples 2–5 are semicrystalline and drawn from sample 1, with sample 4 having the highest draw ratio λ and consequently, at room temperature the highest E (=16.8 GPa). Sample 6 is drawn in one step, has a semicrystalline structure with a degree of crystallinity $\chi = 28\%$ and is the precursor material of sample 7. Sample 8 has a supermolecular structure similar to sample 1 and after a further drawing step leads to the well ordered sample 9 with $\chi = 39\%$.

X-ray investigations

X-ray diffraction experiments with Ni-filtered Cu Kα radiation were used to determine the crystalline chain orientation f_c and χ (ref. 2). The value of f_c was obtained from the $(\bar{1}05)$ WAXS reflection. Considering that the normals of the $(\bar{1}05)$ lattice planes show an angle of 8–10° to the crystalline c-axes[3] an azimuthal angle α was estimated and then f_c according to Stein[4] could be calculated after

$$f_c = (3\langle\cos^2\alpha\rangle - 1)/2 \qquad (1)$$

The value of χ is calculated from the ratio $(L_{\bar{1}05}/L)$ with the crystallite size $L_{\bar{1}05}$ and the meridional SAXS long period L. Assuming a two-phase behaviour the amorphous orientation f_a was calculated according to Samuels[5]:

$$f_a = \frac{\Delta n - \chi\,\Delta n_c f_c}{\Delta n_a(1-\chi)} \qquad (2)$$

where Δn is the measured birefringence, $\Delta n_c = 0.220$ the birefringence of a perfectly oriented crystalline phase and $\Delta n_a = 0.275$ of a perfectly oriented amorphous phase (values obtained from Dumbleton[6]).

Thermo-mechanical investigations

Three different mechanical methods were used to investigate the influence of strain and temperature on the time-dependent mechanical behaviour. First, the static stress–strain behaviour up to the plastic deformation region was studied at different temperatures by using an Instron tensile tester with a deformation speed of

* Present address: IBM Almaden Research, 650 Harry Road, San Jose, CA 95120-6099, USA

0032-3861/92/091881-06

Table 1 Sample characteristics

Samples	E (GPa)	χ (%)	f_c	λ	Δn	f_a
1	8.4	–[a]	–	4.3	0.177	0.644[b]
2	13.4	26	0.98	6.1 4.3 6.5	0.202	0.771
3	15.0	27	0.98	7.0 4.3 7.2	0.228	0.846
4	16.8	33	0.98	7.1 4.3 7.5	0.205	0.727
5	14.3	28	0.98	7.0 4.3 7.3	0.249	0.953
6	7.1	28	0.87	5.4 4.3 5.8	–	–
7	10.2	27	0.96	6.1 4.3 6.3	–	–
8	10.2	–[a]	–	4.2	0.200	0.727[b]
9	12.0	39	0.98	5.3 4.2 5.5	0.219	0.804

[a]Non-crystalline
[b]Other meaning as no two-phase structure exists

$\dot{\varepsilon} = 1\%\ \text{min}^{-1}$. The initial length of the test specimen $l_0 = 100$ mm. The stress σ corresponded to the true stress $\sigma = F/A$, where F is the force and A is the actual cross-section at a certain time. In the region of small deformation the limit of linearity and E were estimated[1]. In order to characterize the irreversible deformation behaviour the yield point estimated from the stress–strain curve, and the irreversible strain ratio $\varepsilon_{iv}/\varepsilon$, calculated from the irreversible part ε_{iv} of a given total strain ε, were used. Further, the time dependence of $\varepsilon_{iv}/\varepsilon$ was measured in retardation experiments.

Second, the relaxation behaviour was studied in the time region of $5\ \text{s} \leqslant t \leqslant 1000$ s at the above temperatures by using the Instron tensile tester. The experiments were carried out at $\varepsilon = 0.5$ and 5.0% (4.0% for sample 4), lying in the viscoelastic or viscoplastic regions, respectively. Values of $l_0 = 100$ mm and $\dot{\varepsilon} = 0.5\%\ \text{min}^{-1}$ were used. The measurement of the relaxation force $F(t)$ started after a loading time of 20 min and an ensuing strain jump of $\Delta\varepsilon_{Re} = -0.2\%$ (back to lower strains). The calculation of the relaxation modulus $E(t)$ was based on the following equation:

$$E(t) = \frac{F(t)}{A\,\Delta\varepsilon_{Re}} \tag{3}$$

where A is the cross-section of the specimen at the relaxation time $t = 0$. From the obtained relaxation curves the relative relaxation strength

$$\Delta E(t) = \frac{E(5\ \text{s}) - E(1000\ \text{s})}{E(5\ \text{s})} \times 100\% \tag{4}$$

was estimated by using $E(t)$ at $t = 5$ and 1000 s.

Third, the dynamic mechanical behaviour was studied with a Rheovibron DDV II and by estimating the temperature dependence of the storage modulus (E'), loss modulus (E'') and loss tangent ($\tan\delta$) at a frequency (f) = 110 Hz.

$$E' = \frac{F_\sim l}{A\,\Delta l_\sim}(1 + \tan^2\delta)^{-1/2} \tag{5}$$

and

$$E'' = E'\tan\delta \tag{6}$$

Here, $\Delta l_\sim$ is the sinusoidal elongation, $F_\sim$ the resulting sinusoidal force and l is the actual specimen length. The heating rate was fixed at 1 K min^{-1}, and the measurements were carried out from room temperature up to 250°C on specimen lengths of $l_0 = 20$ mm.

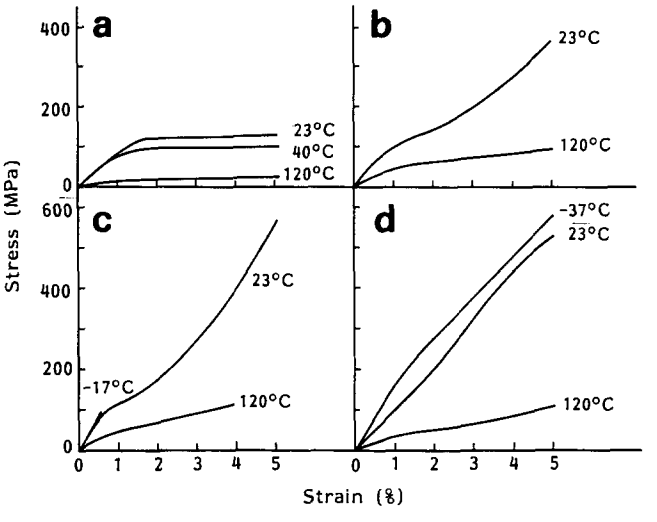

Figure 1 Stress–strain curves for four drawn PET samples: (a) sample 1; (b) sample 2; (c) sample 4; (d) sample 9

RESULTS AND DISCUSSION

Characteristics of the samples

From *Table 1* it can be seen that all drawn samples have a high chain orientation especially in the crystalline phase[2]. The f_c obtained is close to 1.0 and nearly independent of the drawing conditions. In contrast, f_a varies from 0.717 up to 0.953 and depends on the applied drawing stress[1].

Stress–strain behaviour

Using the drawn samples 1, 2, 4 and 9, the principle of the temperature-dependent stress–strain behaviour of highly oriented PET is shown in *Figure 1*. Here, the deformation behaviour is seen both in the viscoelastic and in the viscoplastic regions, but the behaviour at break is not considered. The linear part of the stress–strain curves is approximated by the limit of linearity (stress σ_{lg}, strain ε_{lg}) and E. The viscoplastic behaviour, which occurs at higher strains, is seen from the stress–strain curves and the time dependence of the irreversible strain ratio $\varepsilon_{iv}/\varepsilon$. For all samples investigated and the tem-

Table 2 Results of stress–strain curves at different temperatures

Samples	T (°C)	σ_{1g} (MPa)	ε_{1g} (%)	E (GPa)
0	23	22.5	1.10	2.2
1	23	68.9	0.82	8.4
	40	54.0	0.64	8.4
	120	5.0	0.45	1.2
2	23	67.0	0.50	13.4
	120	26.0	0.48	5.2
3	23	75.0	0.50	15.0
	120	8.0	0.13	5.6
4	−17	>94.0	>0.50	17.5
	23	70.6	0.42	16.8
	120	16.0	0.25	6.0
5	23	72.9	0.51	14.3
6[b]	23	127.1	1.79	7.1
	40	63.0	1.71	3.7
	120	3.7	0.18	2.1
7[b]	23	63.4	0.64	10.2
	120	7.0	0.17	4.4
8	23	66.3	0.65	10.2
	40	27.1	0.36	7.7
	120	3.6	0.35	1.1
9	−37	167.5	0.98	17.3
	23	62.4	0.52	12.0
	120	2.5	0.12	4.8

[a]Non-oriented starting sample[1]
[b]Undulatory macroscopic structure at T = 23 and 40°C

peratures used, the values of E, σ_{1g} and ε_{1g} are listed in *Table 2*.

In general, the stress–strain curves depend on the supermolecular structure. From *Tables 1* and *2* it is seen that at a given χ, an increase in chain orientation can lead to an increase in E at room temperature. This is obtained for the non-crystalline samples 0 (non-oriented), 1 and 8 and for the semicrystalline samples 2, 3 and 7 with $\chi \sim 27\%$. Here, changes from $E = 2.2$ up to 10.2 GPa and from $E = 10.2$ up to 15.0 GPa, respectively, are achieved (*Table 1*). Furthermore, the chain orientation can also influence the strain limit of linearity ε_{1g}. For non-crystalline structures ε_{1g} can decrease from 1.10 to 0.65% with increasing chain orientation. Contrary to that, highly oriented semicrystalline PET structures with $\chi \sim 27\%$ have a constant value of ε_{1g} ($\sim$0.50%). But with increasing crystallinity ε_{1g} can also decrease, as seen for sample 4. Samples 6 and 7 possess an undulatory macroscopic structure at room temperature with $\varepsilon \sim 1.7\%$ for sample 6 and $\varepsilon \sim 0.14\%$ for sample 7[1]. The necessary correction of length can influence ε_{1g} and σ_{1g}. At higher strains above the yield strain ε_y the plastic deformation behaviour also depends on the crystallinity. The higher the χ the smaller are the plastic region and the irreversible strain (*Figure 1*). It can be observed that a temperature rise leads to a decrease both in the limit of linearity (σ_{1g}, ε_{1g}) and in E, as seen in *Table 2*. However, an increase in χ improves the temperature stability, mainly in the plastic deformation region. Consequently, samples 4 and 9 with χ values higher than the other samples show in the deformation range up to $\varepsilon = 5\%$ only small plastic effects at room temperature and at higher temperature a comparatively low decrease in E (*Figure 1*).

Relaxation behaviour

The relaxation experiments are carried out in a time range of 5 s $\leqslant t \leqslant$ 1000 s (*Figure 2*). In general, below the glass transition the $E(t)$ at very short times characterizes the non-relaxed state and consequently, the chain orientation. At higher relaxation times mainly viscoelastic effects occur, but at very long times the $E(t)$ can be strongly influenced by plastic effects due to chain slippage. In order to receive additional information about the deformation behaviour we changed the strain and temperature of the measurement. Using the relaxation curves in *Figure 2* and the results of the stress–strain curves in *Figure 1* it is possible to discuss the time dependence of the reversible as well as the irreversible deformation behaviour. In the case of sample 1 at room temperature (far away from the glass transition temperature T_g = 137°C) the stress–strain curve is linear up to $\varepsilon_{1g} = 0.82\%$. Relaxation experiments at these conditions show that $E(t)$ is time independent for the time region from 5 up to 1000 s (*Figure 2*). Consequently, the total deformation behaviour is either elastic or linearly viscoelastic with very short relaxation times. The same behaviour occurs at 40°C. In contrast, the other drawn samples (2, 4 and 9) in *Figure 2* show viscoelastic behaviour under the above conditions. The stress–strain curves start to deviate from the straight line, and the values of the $E(t)$ decrease slightly with time. At high strains ($\varepsilon = 5\%$) all drawn samples possess irreversible deformation behaviour, which is caused by a chain slippage. From the stress–strain curves it is seen that the applied strain ($\varepsilon = 5\%$) is higher than E_y, which was established according to Ward[7].

Furthermore, we discuss the strain dependence of the short-time relaxation modulus $E(t = 5\text{ s})$ and the long-time relaxation modulus $E(t = 1000\text{ s})$. At small strains and temperatures below the glass transition, where the product of frequency and relaxation time is $\omega\tau_i \gg 1$, practically no changes in viscoelastic properties occur within the period of deformation[8]. This behaviour can be investigated by measuring $E(t)$ at different times and temperatures. In relaxation experiments at T = 23 and −17°C where the molecular mobility is nearly frozen[9], sample 4 shows that $E(t = 5\text{ s})$ at $\varepsilon = 0.5\%$ is nearly time independent and can be used to characterize the chain orientation (*Figure 2*).

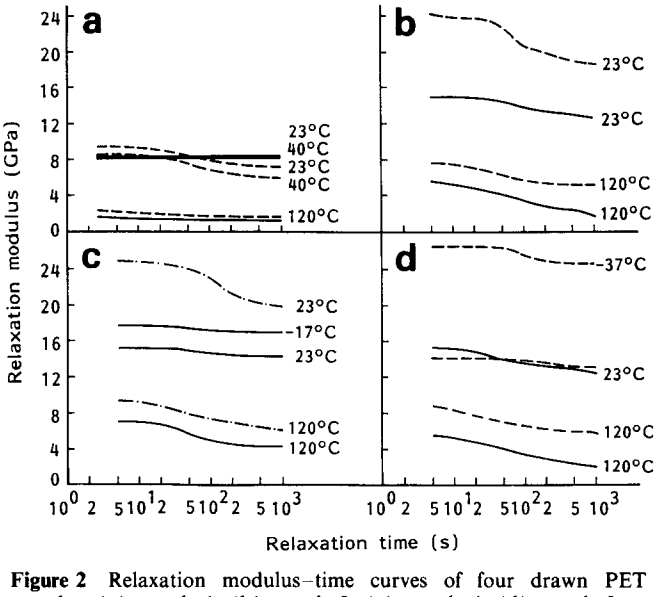

Figure 2 Relaxation modulus–time curves of four drawn PET samples: (a) sample 1; (b) sample 2; (c) sample 4; (d) sample 9. ε: (——) 0.5%; (—·—) 4%; (– – –) 5%

Table 3 Results of relaxation experiments

Samples	T (°C)	ε (%)	$E(t = 5\,s)$ (GPa)	$E(t = 1000\,s)$ (GPa)	$\Delta E(t)$ (%)
1	23	0.5	8.3	8.3	0.0
		5.0	9.4	7.0	25.5
	40	0.5	8.3	8.3	0.0
		5.0	8.5	5.8	31.8
	120	0.5	1.6	1.2	25.0
		5.0	2.2	1.5	31.8
2	23	0.5	14.9	12.6	15.4
		5.0	24.0	18.5	22.9
	120	0.5	5.6	1.8	67.9
		5.0	7.6	5.2	31.6
4	−17	0.5	17.7	16.8	5.1
	23	0.5	15.1	14.2	6.0
		4.0	24.8	19.7	20.6
	120	0.5	7.0	4.3	38.6
		4.0	9.3	6.2	33.3
9	−37	5.0	26.5	24.6	7.2
	23	0.5	15.3	12.5	18.3
		5.0	14.2	12.9	9.2
	120	0.5	5.6	2.3	58.9
		5.0	8.8	6.3	28.4

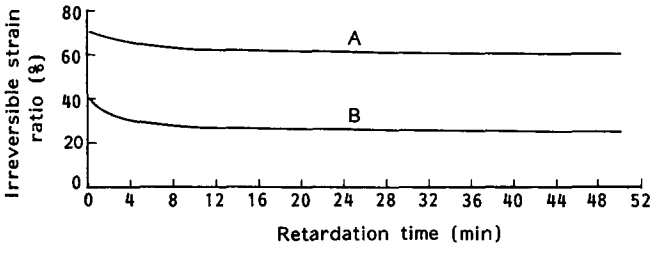

Figure 3 Dependence of the irreversible strain ratio on time for two drawn PET samples measured at $\varepsilon = 10\%$ and $T = 23°C$: (A) sample 1; (B) sample 9

In the case of the semicrystalline samples 2 and 4 $E(t = 5\,s)$ increases in the deformation region $0.5\% \leqslant \varepsilon \leqslant 5.0\%$ with rising strain. (For sample 4 the upper limit $\varepsilon = 4\%$ is used because of the tendency to break[1].) This increase in $E(t = 5\,s)$ shows that the established viscoplastic effects at higher strains $1.5\% \leqslant \varepsilon \leqslant 5.0\%$ can only be small. In contrast, the non-crystalline sample 1 changes its deformation behaviour strongly in the above region and at $\varepsilon \geqslant 1.8\%$ a large chain slippage occurs[1]. This produces a decrease in the achievable chain orientation and consequently, a lower $E(t = 5\,s)$ (*Table 3*).

At low strains the deformation behaviour of the semicrystalline sample 9 is similar to that of samples 2 and 4, but at $\varepsilon \geqslant 4.5\%$ large viscoplastic effects occur. These effects already take place during the loading prior to the start of the relaxation measurement. That is why at room temperature $E(t = 5\,s)$ is lower at $\varepsilon = 5.0\%$ than at $\varepsilon = 0.5\%$ (*Figure 2*). Furthermore, it is seen for sample 9 that very low temperatures decrease the chain slippage. Consequently, experiments at $T = -37°C$ and $\varepsilon = 5\%$ show a very high $E(t = 5\,s) = 26.5$ GPa (compared with 14.2 GPa at room temperature) and a low $\Delta E(t)$ (*Table 3*).

The $E(t = 1000\,s)$ contains viscoelastic and viscoplastic effects. The samples with a strong chain slippage (at $T = 23°C$ sample 1 at $\varepsilon \geqslant 1.8\%$ and sample 9 at $\varepsilon \geqslant 4.5\%$) possess only a low $E(t = 1000\,s)$. In addition retardation experiments at room temperature at a total strain $\varepsilon = 10\%$, the viscoplastic deformation behaviour is investigated. *Figure 3* shows the time dependence of the irreversible strain ratio $\varepsilon_{iv}/\varepsilon$ of typical viscoplastic behaviour, typified by samples 1 and 9. After a retardation time of $t = 1000\,s$ the ratios $\varepsilon_{iv}/\varepsilon = 61\%$ for sample 1 and 26.5% for sample 9 are obtained.

With rising temperature the molecular processes will be stimulated and consequently, the $E(t)$ decreases, depending on the existing supermolecular structure. In *Figure 2* it is seen that the crystallinity strongly influences the relaxation behaviour at higher temperatures. High temperatures and a low crystallinity favour the existence of chain slippage. In case of a large slippage $\Delta E(t)$ can vanish (see sample 1).

Dynamic-mechanical behaviour

The dynamic-mechanical investigations are carried out in the temperature region of $23°C \leqslant T \leqslant 250°C$ and at a very small strain lying in the linear viscoelastic deformation region. At room temperature ($T = 23°C$) PET is in a glassy state, independent of the existing supermolecular structure, and the molecular mobility is nearly frozen. As is seen in *Figure 4*, the drawn samples differ strongly in their E' values at room temperature. Mainly, this is due to the chain orientation obtained after drawing[10,11] (*Table 1*). The highest E' is achieved for sample 4 with $E' = 19.3$ GPa (*Table 4*).

In the temperature region from room temperature up to 50°C the $\tan\delta$ of all samples investigated is smaller than 0.017. Such low values are typical for an elastic deformation behaviour[11]. Furthermore, in the above temperature region the E' of all drawn samples changes slowly with increasing temperature and hence, the sample stiffness remains nearly constant (*Figure 4*). With a further rise in temperature the samples investigated show an α-dispersion, which is characterized by a large peak in the E'' curve. In the case of PET this α-dispersion is due to the micro-Brownian motion of large molecular segments in the amorphous regions[12]. Depending on the supermolecular structure after drawing, the temperature position of the E'' maximum, referred to as T_g, as well as the peak area can be discussed. It is known that T_g corresponds to the mobility of molecular chains and hence, a shift to higher temperatures indicates that the mobility is hindered by changes of the supermolecular structure. In the following, the influence of orientation and crystallinity on T_g will be discussed. The results show that for non-crystalline PET, the T_g rises strongly with increasing chain orientation. For example, T_g increases from 82°C (non-oriented structure) to 137°C (sample 1), and eventually to 142°C (sample 8). For semicrystalline structures the molecular mobility is additionally hindered by crystallization effects and hence the T_g is somewhat higher than that of a non-crystalline structure[11]. In the case of highly oriented PET samples with a crystallinity of ~27%, very high T_g values between 154°C and 168°C are measured (*Table 4*). Here, changes of the chain orientation yield only small changes of T_g. For example, the comparison of the semicrystalline samples 6 and 7 or 2 and 5, having nearly the same crystallinity, shows a small T_g increase of ~5 K with increasing chain orientation. In the following, depending on the chain orientation we measure the influence of the crystallinity on T_g. For the two highly oriented samples 2 and 8, having nearly the same chain orientation, it is established

Table 4 Results of dynamic-mechanical experiments

Samples	E'(24°C) (GPa)	E'(230°C) (GPa)	$\frac{E'(230°C)}{E'(24°C)}$ (%)	$T_g = T_{E'',max}$ (°C)	S (K)	Tan δ (24°C)	$T_{\tan\delta,max}$ (°C)	Tan δ, max
1	8.7	0.6	7	80/137	34.4	0.013	79/150	0.174
2	14.7	4.2	29	162	58.3	0.014	174	0.069
3	15.6	4.4	28	152	56.7	0.012	165	0.073
4	19.3	4.9	25	158	54.0	0.010	170	0.077
5	15.6	4.8	31	168	64.9	0.015	182	0.070
6	–[a]	3.1	–[a]	154	53.2	0.016	166	0.077
7	13.2	3.9	29	159	60.6	0.011	172	0.064
8	9.3	0.7	7	54/142	38.7	0.010	55/155	0.139
9	13.7	2.9	21	150	50.5	0.010	160	0.078

[a]Because of undulatory macroscopic structure no value exists at $T = 24°C$

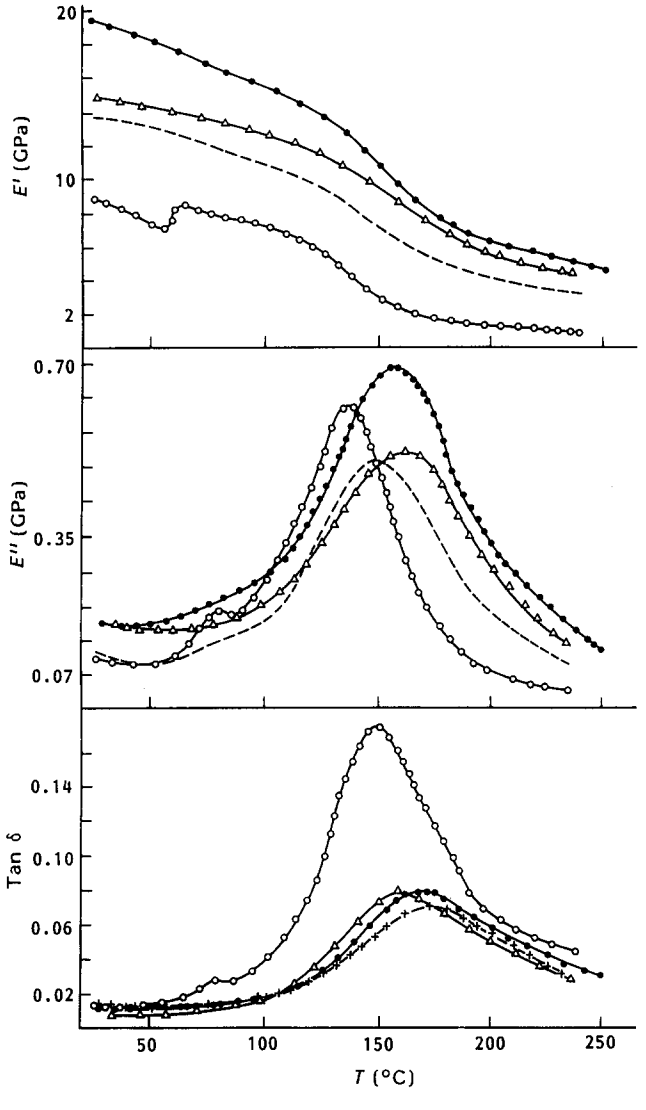

Figure 4 Dependence of the storage modulus (E'), loss modulus (E'') and loss tangent (tan δ) on the temperature (T) of four drawn PET samples: (○) sample 1; (△) sample 2; (●) sample 4; (+) sample 9

that the semicrystalline sample 2 with $\chi = 26\%$ has a T_g which is 20 K higher than the T_g of the non-crystalline sample 8. This result corresponds to the known fact that an increase in the crystallinity will shift T_g to higher temperatures[13]. However, it is also seen that the semicrystalline samples 2, 4 and 9, having nearly the same high chain orientation, show a decrease in T_g up to $\Delta T = 12$ K with increasing crystallinity (*Table 4*).

Regarding the peaks of E'' and tan δ in *Figure 4*, it can be established that the shape of the peaks depends on the supermolecular structure. It is known that the height of the E'' dispersion peak is proportional to the quantity of energy dissipated as frictional heat per cycle in a sinusoidal deformation[8] and that the peak width characterizes a possible hindering of the molecular mobility[14]. Consequently, after drawing the non-crystalline PET, a tall and narrow E'' dispersion peak is observed compared to the semicrystalline sample. The half width (S) values of the E'' peak are 34.4 and 38.7 K (*Table 4*) for the highly oriented non-crystalline samples 1 and 8, respectively. In contrast, the drawn semicrystalline samples show a greater S (between 50.5 K and 64.9 K). The dimensionless parameter $\tan\delta = E''/E'$, which is the ratio of energy lost to energy stored in a cyclic deformation, can be discussed in analogy to the behaviour of E''. For non-crystalline PET it is established with increasing chain orientation that $\tan\delta_{max}$ of the α-dispersion decreases from $\tan\delta_{max} > 1.0$ for isotropic structures to $\tan\delta_{max} = 0.139$ for highly oriented structures. The highly oriented semicrystalline structures possess much lower values of $\tan\delta_{max} \sim 0.07$.

In the temperature region between room temperature and T_g the non-crystalline but highly oriented samples 1 and 8 show an additional dispersion region at 80 and 54°C, respectively. The sample with the higher chain orientation displays the dispersion region at the lower temperature (*Figure 4*). The value of E' increases by a step in this dispersion region and hence E' deviates from normal behaviour. Such an effect has also been found by Schröder[11] and Boyer[15], but up till now the molecular mechanism has not been clarified. Our experiments (d.s.c., X-ray, Fourier transform i.r., shrinkage and temperature-dependent birefringence) lead to the conclusion that this peak is caused by two temperature-stimulated processes: orientation relaxation and simultaneous crystallization. These results will be published later.

CONCLUSIONS

This report continues the discussion of producing highly oriented PET samples by drawing[1] and the resulting

supermolecular structures[2]. Stress–strain curves have shown that highly drawn PET samples possess a strongly reduced plastic deformation behaviour. But already at low strains ($\varepsilon \sim 0.5\%$) plastic effects can occur. Measurements at room temperature show for drawn PET samples that an increase in the chain orientation leads to an increase in E and additionally for non-crystalline samples a decrease in ε_{lg}. Relaxation experiments in a time range of $5\text{ s} \leqslant t \leqslant 1000\text{ s}$ by varying the strain and the temperature are used to investigate the time-dependent reversible and irreversible deformation behaviour. At low strains ($\varepsilon \leqslant 0.5\%$) and $T < T_g$ nearly time-independent behaviour is established. Here, $E(t = 5\text{ s})$ rises with increasing chain orientation, while higher strains ($\varepsilon > 0.5\%$) can yield chain slippage. Very low temperatures (e.g. $T = -37°C$) decrease the chain slippage at higher strains and consequently, extremely high $E(t = 5\text{ s})$ and low $\Delta E(t)$ are achievable. In dynamic-mechanical investigations at sufficiently low strains ($\varepsilon \leqslant 0.1\%$) only very low tan δ values are measured in the temperature region between 23°C and 50°C, which is due to an elastic behaviour. At higher temperatures $137°C \leqslant T \leqslant 168°C$ an α-dispersion with a large peak in the E'' curve is obtained. Depending on the supermolecular structure after drawing, the temperature position of the E'' maximum (T_g) as well as the peak shape and the peak area are discussed. It is found that for non-crystalline PET the T_g rises with increasing chain orientation from 82 up to 142°C. In the case of highly semicrystalline samples with $\chi = 27\%$ very high T_g values between 154°C and 168°C are measured. For highly oriented PET an increase in the crystallinity shifts T_g to higher temperatures, but also a decrease in T_g up to $\Delta T = 12\text{ K}$ is established. Additional to the glass transition, highly oriented non-crystalline PET shows a dispersion region lying below T_g. This can be due to orientation relaxation processes connected with a simultaneous improvement of the molecular order.

REFERENCES

1 Göschel, U. *Acta Polym.* 1989, **40**, 23
2 Hofmann, D., Göschel, U., Walenta, E., Geiß, D. and Philipp, B. *Polymer* 1989, **30**, 242
3 Gupta, V. B., Ramesch, C., Patil, N. B. and Chidambareswaran, R. K. *J. Polym. Sci., Polym. Phys. Edn.* 1983, **21**, 2425
4 Stein, R. S. *J. Polym. Sci.* 1958, **31**, 327
5 Samuels, R. J. *J. Polym. Sci. A2* 1965, **3**, 1741
6 Dumbleton, J. H. *J. Polym. Sci. A2* 1968, **6**, 795
7 Ward, J. M. 'Mechanical Properties of Solid Polymers', J. Wiley & Sons Ltd, London, 1971
8 Ferry, J. D. 'Viscoelastic Properties of Polymers', John Wiley & Sons, New York, 1980
9 Thompson, A. B. and Woods, D. W. *Trans. Faraday Soc.* 1956, **52**, 1383
10 Kunugi, T., Ichinose, C. and Suzuki, A. *J. Appl. Polym. Sci.* 1986, **31**, 429
11 Schröder, H. U. *PhD Dissertation* TH Aachen, 1978
12 Dobbert, P., Krämer, L., Mischok, W. and Zelenev, Ju. *Acta Polym.* 1984, **35**, 89
13 Dumbleton, J. H., Bell, J. P. and Murayama, T. *J. Appl. Polym. Sci.* 1968, **12**, 2491
14 Chang, M. C. O., Thomas, D. A. and Sperling, L. H. *J. Appl. Polym. Sci.* 1987, **34**, 409
15 Boyer, R. F. *J. Macromol. Sci.* 1973, **B8**, 503